npj | heritage science

Article

https://doi.org/10.1038/s40494-026-02319-8

Dynamic response prediction and safety assessment of suspended ancient wooden structures under tourist-induced pedestrian loads

Check for updates

Ruiling Zhang[1,2], Miaole Hou[1,2], Xianglei Liu[1,2], Youqiang Dong[1,2] ✉, Junxiao He[1], Yang Deng[1], Jingshu Wu[3] & Xiaobin Bai[3]

Suspended ancient timber structures, characterized by complex construction and unique load-transfer mechanisms, are prone to pronounced dynamic responses under pedestrian walking loads. This study aims to systematically investigate the structural responses from both deterministic and stochastic perspectives. Graded vertical loading tests were conducted to reveal the mechanical behavior and safety redundancy of the structure under pedestrian loads. Based on a stochastic load model, a comprehensive crowd–structure interaction model was developed by incorporating step-frequency synchronization, spatial coherence, and weak crowd–structure coupling effects, enabling accurate prediction of vibration responses. Monte Carlo simulations were employed to evaluate dynamic responses and explore the nonlinear relationship between pedestrian numbers and structural behavior. A parametric prediction model with 95% accuracy was established, allowing reliable response prediction and safety warning. Finally, safety prediction and graded pedestrian control strategies are proposed to support refined protection, intelligent monitoring, and visitor management of such heritage structures.

Suspended ancient wooden structures are often built against steep cliff faces to expand usable space within extremely limited terrain. As a result, their corridors and platforms are typically narrow, with passage widths allowing passage for only one or two people side by side. While this compact layout creates a unique touring experience characterized by "changing views with every step" and a sense of exploration, it inevitably restricts pedestrian flow efficiency and evacuation capacity. Due to these confined pathways, bidirectional movement is difficult to achieve, making one-way circulation routes not only a management necessity but also a spatial constraint. Visitors follow a prescribed unidirectional path, which means that congestion at any point can quickly propagate throughout the system. With the growing popularity of heritage tourism, these suspended structures attract increasing numbers of visitors. During peak periods, dense crowds in such confined spaces can induce significant dynamic structural responses. More critically, in emergencies such as fires or strong winds, the limited evacuation routes heighten the risk of severe congestion and serious safety hazards[1]. In extreme cases, dynamic effects induced by crowd loads may even lead to structural instability or collapse[2]. Therefore, thoroughly understanding and accurately predicting pedestrian-induced loads on suspended ancient timber structures has become an essential prerequisite for ensuring structural safety, long-term usability, and preventive conservation[3,4].

Vibration serviceability assessment plays a crucial role in ensuring the comfort and safety of building occupants. Current guidelines for evaluating structural vibration responses induced by human walking loads[5,6] typically rely on simplified approaches that model pedestrians as independent moving load sources and employ deterministic step frequencies with simplified harmonic functions to compute structural responses[7,8]. However, several studies have highlighted limitations and shortcomings in these guideline methodologies[9,10]. To address these limitations, researchers have gradually introduced probabilistic approaches. For instance, Demartino et al.[11] conducted a numerical study on footbridge vibrations induced by a single pedestrian, proposing both deterministic and probabilistic methods for vibration serviceability assessment. Picozzi et al.[12] proposed a reliability quantification method that accounts for the variability in pedestrian walking loads and uncertainties in footbridge properties, establishing design response spectra for vertical and lateral vibrations. While such studies

[1]Beijing University of Civil Engineering and Architecture, Beijing, China. [2]Beijing Key Laboratory for Architectural Heritage Fine Reconstruction & Health Monitoring, Beijing, China. [3]China Inspect & Certificat CO LTD, MCC, Beijing, China. ✉e-mail: dongyouqiang@bucea.edu.cn

provide fundamental vibration response data, their practical applicability remains limited due to the greater complexity of real crowd loading conditions. Specifically, single-person excitation models fail to adequately simulate the combined effects of multiple pedestrians walking simultaneously with different gait patterns, leading to limited representativeness of the results under actual crowd load conditions[13,14].

The vibration response under multiple pedestrian excitations is often greater than that under a single pedestrian excitation[15,16]. Wang et al.[17,18] suggested approach to predict the human-induced vibration of Cross-Laminated Timber (CLT) floors was based on multi-person loads. They also proposed a temporary spectral model to analyze crowd loads on building floors. However, this approach also has limitations, including the assumption that pedestrians are stationary individuals and the neglect of variations in walking paths. These constraints may potentially limit its practical applicability in real-world scenarios[19].

Considering the randomness of actual walking load scenarios and walking paths, Georgakis et al.[20] proposed a response spectrum method to calculate the peak acceleration response of pedestrian bridges. By adopting a probabilistic walking load model and performing a series of Monte Carlo simulations, a reference response spectrum was established. Piccardo et al.[21] introduced an equivalent spectral model to analyze the dynamic response of pedestrian bridges under normal, unrestricted pedestrian traffic while accounting for random excitation sources. Building on existing pedestrian bridge models, Bayat et al.[22] proposed an analytical expression for the equivalent power spectral density function of modal forces. In addition, they derived a formula for calculating the mean peak acceleration response of floors. These methods, which consider the influence of random factors, can enhance the accuracy and reliability of structural vibration suitability assessments.

However, the load-bearing system of suspended ancient timber structures exhibits notable specificity and complexity. The main load-bearing timber beams are embedded at one end into the mountain rock. Due to limited embedment depth and the slippage and rotation at the rock–timber interface, a semi-rigid embedded boundary is formed, resulting in relatively low overall structural stiffness and granting the structure a certain degree of deformability and energy dissipation capacity. Meanwhile, the narrow passageways not only restrict free pedestrian movement but also promote significant step-frequency synchronization and path-coupling effects in high-density crowds. Furthermore, stiffness degradation due to timber aging, the semi-rigid behavior of mortise–tenon connections, and variations in historical construction techniques collectively constitute the distinctive dynamic system foundation of such structures.

Existing stochastic crowd load models typically rely on assumptions such as independent pedestrian motion and normally distributed step frequencies and lengths, making it difficult to accurately characterize the specific dynamic behavior of such ancient timber structures and their coupling mechanisms with crowds. Particularly in cases where structural flexibility is significant, and boundary conditions are complex, existing models neither adequately account for the influence of time-dependent structural properties on system frequency and damping, nor do they effectively represent high-density crowd phenomena such as synchronization behavior, spatial coherence, and human–structure dynamic feedback (e.g., step-frequency lock-in and gait adaptation). Moreover, the approach of simply superimposing single-pedestrian loads to simulate collective crowd behavior proves insufficient in the confined spaces of heritage structures, where pedestrian motion is highly correlated and structural dynamic characteristics are complex.

To address these limitations, this study proposes an improved human–structure dynamic interaction model. Within the framework of traditional stochastic load modeling, the model systematically incorporates step-frequency synchronization effects, spatial coherence functions, and weak human–structure coupling mechanisms. By equivalently modeling key characteristics such as timber aging and semi-rigid joint behavior, the model more realistically reflects the coupled dynamic behavior between dense crowds in confined spaces and flexible ancient timber structures. This model aims to reveal the vibration response mechanisms of suspended ancient timber structures under crowd loading and provides a more tailored numerical analysis tool for evaluating their vibration comfort and long-term safety performance, specifically adapted to the features of heritage structures.

Furthermore, existing studies offer very limited measured data under high-density conditions, and current design codes lack specific vibration limits or risk thresholds tailored to cultural heritage structures[23]. Based on this, this study takes suspended ancient wooden buildings as the object, and the innovation and contribution of the research are mainly reflected in the following aspects:

- Unlike previous studies focusing on main load-bearing components, this research quantitatively reveals through graded vertical loading tests and mechanical coupling analysis, the implicit safety redundancy mechanism of wooden columns under crowd loads: although not significantly sharing main beam stresses, they effectively suppress structural displacement, thereby enhancing overall structural deformation controllability. This finding advances the conventional understanding of "non-load-bearing components" in conservation practice, providing new scientific basis for integrated structural behavior control of suspended ancient timber structures.
- Aiming at the limitations of existing stochastic crowd load models in representing pedestrian behavior within narrow passageways, this study innovatively develops an integrated crowd-structure interaction model that incorporates step-frequency synchronization, spatial coherence, and weak structure-pedestrian coupling mechanisms. The model systematically reveals the intrinsic relationship between crowd density and structural acceleration response and, further, proposes critical crowd density thresholds for safety warning and comfort management from the dual perspectives of structural safety and pedestrian comfort. This model overcomes the analytical limitations of traditional stochastic load models and provides key quantitative management criteria for preventing structural resonance overload risks and ensuring normal serviceability comfort.

Methods

Features of suspended ancient wooden structure

The suspended ancient structure is built along the cliffs, closely integrated into the mountain terrain. The Suspension wooden boardwalk connects the various pavilions of the temple. The design cleverly takes into account the height difference between the pavilions and uses a slope transition to ensure convenience and comfort for tourists. The wooden structures are made of pine wood and treated with tung oil, making it durable and structurally stable. It can effectively resist the erosion of the natural environment while being both practical and beautiful. As shown in Fig. 1.

The main structure of the wooden boardwalk is composed of wooden beams and wooden columns. These components are tightly connected by mortise and tenon joints to form a solid structure. The wooden beams are placed horizontally and serve as the main load-bearing structure of the wooden boardwalk. The wedge design at one end of the wooden beam allows it to be fastened after being inserted into a stone hole with a large inside and a small outside. This method is equivalent to the modern "expansion screw" and supports the weight of the wooden boardwalk. As shown in Fig. 2, the bottom of the wooden column is embedded in the rock and fixed by drilling holes. Under normal circumstances, the wooden column does not directly bear the weight of the wooden boardwalk. However, when tourists walk across, it provides additional support, turning the bridge from a "statically determinate structure" to an "over-statically determinate structure" capable of bearing walking loads. The wooden boardwalk consists of wooden boards laid on the wooden beams, with wooden railings on either side of the road. These railings not only ensure people's safety, but they also add a decorative element that is harmonious to the Temple's overall architectural style.

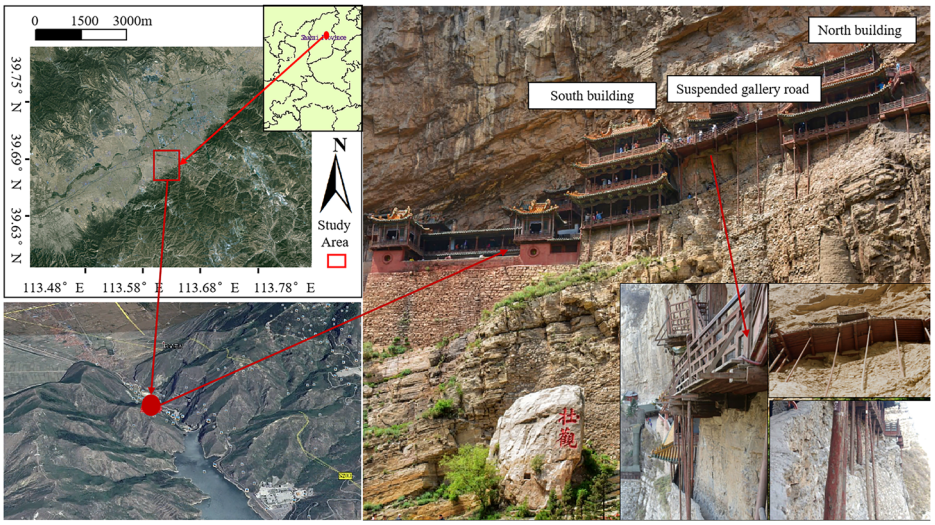

Fig. 1 | Suspended AQ6 wooden boardwalk structure. The Hanging Temple's geographical location and structural form.

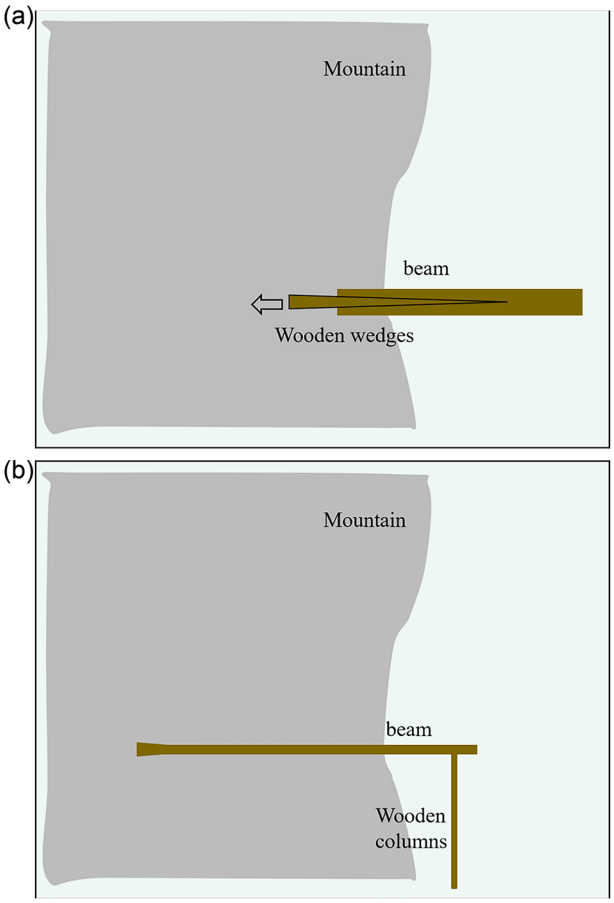

Fig. 2 | Suspended wooden boardwalk structure construction techniques. **a** Anchoring the crossbeam by embedding its end into the mountain body. **b** Connecting the cantilevered end of the crossbeam to the wooden column.

Reverse reconstruction

This study takes the wooden boardwalk of Mount Heng as the research object. Using a NavVis MLX handheld 3D laser scanner, integrated interior and exterior data acquisition of the entire Hanging Temple complex was conducted, obtaining high-precision, continuous 3D point cloud data. During point cloud preprocessing, the walkway structure was segmented into four categories of semantic components: pillars, beams, deck panels, and railings, achieving component-level spatial identification and data decoupling. Key geometric parameters of the components were subsequently extracted based on the segmentation results, including span, cross-sectional dimensions, joint locations, and spatial orientations, for 3D solid model reconstruction.

To address the issue of missing point clouds caused by partial occlusion of the wooden boardwalk, this study performed geometric inference and completion of hidden structures based on traditional timber joinery (mortise-and-tenon) techniques. In the beam-column connection zones, concealed features such as hidden tenons and mortises were identified and reconstructed by supplementing the geometric relationships of the joints, thereby achieving an authentic representation of the component connections. Furthermore, geometric dimensions, timber material properties (e.g., elastic modulus and density of hemlock), structural connection types, and spatial topological relationships were integrated into the Building Information Modeling (BIM) geometric model and structural database. This provides complete input conditions for subsequent finite element analysis, realizing end-to-end parametric continuity throughout the entire workflow from point cloud acquisition and geometric modeling to mechanical simulation[24–27]. The specific modeling workflow is shown in Fig. 3.

Finite element static analysis model to determine tourist-induced pedestrian loads

The BIM model was exported in IGES format and imported into ABAQUS for finite element simulation. Historical records and on-site investigation indicate that the wooden walkway is primarily constructed of hemlock wood. Based on data from relevant literature, the mechanical properties of hemlock are summarized in Table 1, showing a density of 0.506 g/cm^3, which indicates a material with relatively high stiffness and strength. Considering the structure's long service period since its last reconstruction and its status as a cultural heritage site, the effects of long-term loading, material aging, and service-induced degradation were accounted for. In accordance with relevant code provisions, a reduction factor of 0.90 was applied to the elastic modulus to reflect the actual in-service mechanical condition. To accurately obtain the stress and displacement distributions of the deck and identify potential stress concentration areas, the entire structure was discretized using solid elements for meshing and numerical analysis. The beam extends 1 m into the cliff wall, with constraints applied to its vertical and lateral displacements. The beam-plate contact was modeled as a fixed connection. To investigate the load-bearing contribution of the wooden columns, two working conditions were designed: Condition 1, where the column base is hinged, and the beam-column interaction is defined by tangential and

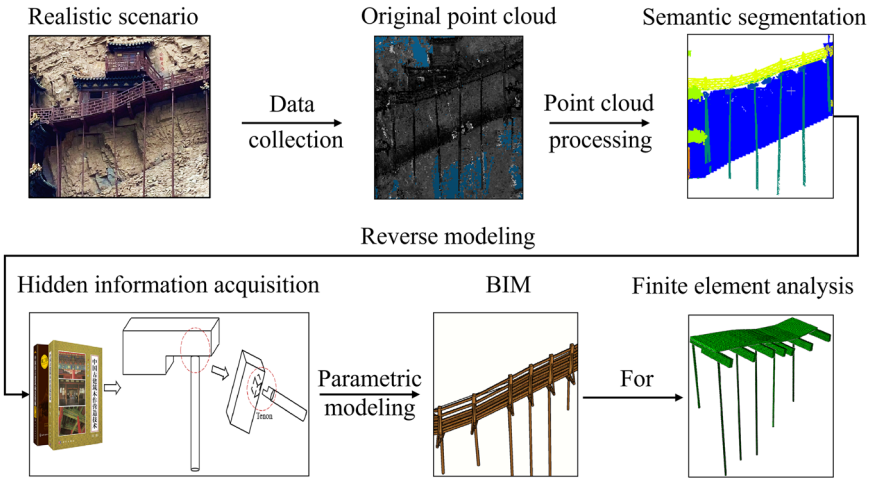

Fig. 3 | Parametric modeling technology process. A reverse engineering workflow for the wooden boardwalk based on point cloud data.

Table 1 | Physical and mechanical properties of hemlock wood

$E_{C,L}$	$E_{C,R}$	$E_{C,T}$	$f_{C,L}$	$f_{C,R}$	$f_{C,T}$
11509	890	493	38.1	3.3	2.9
μ_{LR}	μ_{LT}	μ_{RT}	G_{LR}	G_{LT}	G_{RT}
0.54	0.46	0.40	829.4.	663.5	199.1

$E_{C,L}$, $E_{C,R}$, $E_{C,T}$ represent the compressive elastic modulus of wood in the smooth grain, transverse radial, and transverse diagonal directions, respectively. $f_{C,L}$, $f_{C,R}$, $f_{C,T}$ denote the compressive strength of wood in the smooth grain, transverse radial, and transverse chordal directions, respectively. μ_{LR}, μ_{LT}, μ_{RT} are the Poisson's ratio of wood in radial, chordal, and transverse sections, respectively. G_{LR}, G_{LT}, G_{RT} represent the shear modulus of wood in radial, chordal, and transverse sections, respectively. The unit of strength is MPa.

hard contact behavior; and Condition 2, without wooden columns at the beam ends. The resulting finite element model is shown in Fig. 4.

Crowd-structure interaction (CSI) model

Human walking is a periodic cyclic motion, starting from one foot touching the ground until the same foot touches the ground again to complete a complete gait cycle. Each step will generate a periodic impact force on the structure, which is composed of the static effect of the body weight and the dynamic effect of walking. The static effect can be approximated as a constant gravity load, while the dynamic effect is a periodic change, which can usually be decomposed into multiple harmonic components by Fourier series to describe the main frequency characteristics of the walking force. In the behavior induced by tourists, vertical, lateral and longitudinal dynamic loads act together, among which the vertical force is usually considered to have the greatest impact on the structure, so it has become the focus of research. In order to more accurately simulate the dynamic load in the vertical direction, the classic single tourist loading model is introduced, and the multi-frequency superposition model is introduced into the statistical distribution characteristics of the pedestrian step frequency. The total load can be expressed as:

$$F_{total}(t) = G + \sum_{i=1}^{N} Ga_i \sin(2\pi i f_p^t + \varphi_i) \quad (1)$$

Where G is the weight of the tourist, i is the order of the harmonic, α_i is the Fourier coefficient of the ith harmonic, called the dynamic load factor, f_p is the step frequency, φ is the walking harmonic phase angle.

The model combines the Fourier series and the statistical distribution characteristics of the step frequency, uses a multi-frequency superposition method to describe the walking-induced force, and focuses on the main harmonic components in the force spectrum, so as to more realistically reflect the dynamic impact of tourists walking on the structure. However, under the deterministic analysis framework, traditional models often have difficulty in fully describing the randomness and time-varying characteristics of tourist-induced pedestrian loads, and in accurately reflecting their dynamic impact on structures. Therefore, it is crucial to introduce a spatiotemporal model, which describes the time-varying distribution and spatial action characteristics of tourist-induced pedestrian loads by constructing time and space functions, thereby more comprehensively revealing the impact mechanism of tourist groups on structural responses.

The Heaviside step function can describe the impact load or vibration load applied over a period of time. Mathematically defined as When $t < 0$, $H(t) = 0$, and when $t > 0$, $H(t) = 1$. When $t = 0$, it may be defined as 0.1 or 0.5 according to different requirements. As shown in the Fig. 5a.

Pedestrian groups are represented as a dynamic collection of discrete action points in space, as shown in Fig. 5b. Pedestrian walking behavior has significant random characteristics. The step length, step frequency and path selection are all affected by individual differences and environmental factors. Assuming that pedestrians only move in the positive direction along the parallel line of the x-axis during movement, in order to reasonably express this characteristic, the dual-scale single-person walking load $F(t)$ based on time and space is expressed as:

$$\begin{aligned} F_{total}(t) &= G + \sum_{i=1}^{N} Ga_i \sin\left(2\pi i f_{p,i} t + \varphi_i\right) \\ x_t &= x_0 + v_x t \\ y_t &= y_0, 0 \le t \le \sum_{i=1}^{\beta} t_i \end{aligned} \quad (2)$$

To this end, the Dirac delta function $\delta(x\text{-}x_0)$ is used to limit the action area of the force in space, and the Heaviside function $H(t\text{-}t_0)$ is used to limit the action period of the force in time. Based on the single person load $F(t)$, the crowd load in the spatiotemporal random distribution model is expressed according to the superposition principle as follows:

$$\begin{aligned} F(x,t) = \sum_{i=1}^{N_p} \sum_{h=1}^{N_h} G_i a_{h,i} \sin(2\pi h f_{p,i} t + \phi_{h,i}) \delta\left(x - x_{p,i}(t)\right) \\ \left[H(t-\tau_i) - H\left(t - \tau_i - \frac{L_{wpi}}{v_i}\right)\right] \end{aligned} \quad (3)$$

where, Np and N_h denote the total number of tourists and walking harmonic; $\alpha_{h,i}$ is dynamic load factor; δ is Dirac delta function; h is the order number of harmonic of pacing rate ; τ_i is the arrival time; L_{wpi} is the length of the walking path; v_i is the walking speed of the ith tourist; $x_{p,i}$ is the

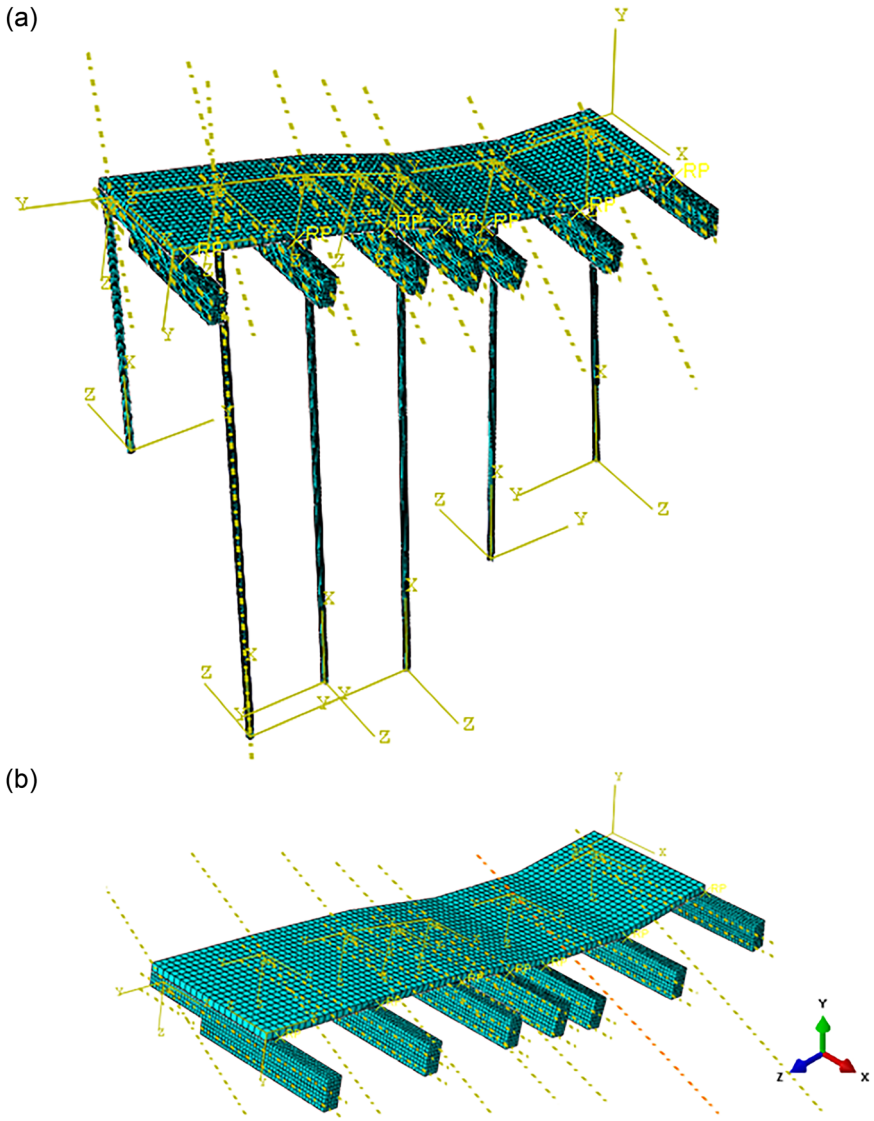

Fig. 4 | Finite element model of working condition 1 and working condition 2. a Condition 1. **b** Condition 2.

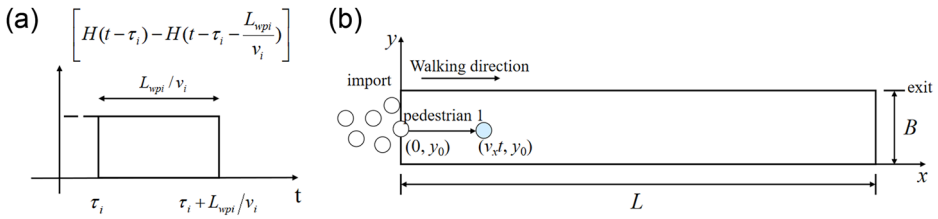

Fig. 5 | Schematic of the mathematical and load models used in the simulation. a Heaviside step function used to regulate the application of force. **b** Schematic diagram of the pedestrian load model applied on the structure.

location reached by the tourist at time *t*. This formula fully considers the load impact of multiple tourists on the structure, and sums the number of tourists and the harmonic components respectively through the double summation symbol, reflecting the diversity of the number of tourists and the complexity of the walking load.

Pedestrian dynamic parameters such as step frequency and walking speed are not isolated variables but exhibit significant nonlinear characteristics that vary with crowd density. At low densities (typically below 1.0 pers./m^2), individuals maintain considerable spacing and are in a state of free walking. Their parameters, including step frequency and stride length, are primarily determined by personal habit, walking purpose, and environmental layout, and can be treated as mutually independent random variables. Under these conditions, traditional stochastic load models, which assume normal distributions for step frequency and stride length and superimpose them independently, can effectively simulate crowd loads.

However, as density increases and available space diminishes, pedestrian movement becomes constrained, manifesting trends of collective synchronization and spatial coherence. In this regime, the limitations of traditional independent stochastic models become apparent:

(1) Enhanced step-frequency synchronization: Pedestrian step frequencies are influenced by neighboring individuals and tend to converge, making complete independence unsustainable.
(2) Significant spatial coherence: The footfall impacts of adjacent or nearby pedestrians show correlations in both time and space.

(3) Emergence of crowd-structure interaction: Structural vibrations can provide feedback that influences pedestrian gait, potentially triggering phenomena such as "frequency lock-in" or gait adaptation, thereby altering the input loading.

To overcome these limitations, this study introduces an integrated crowd-structure interaction mechanism into the stochastic load framework, aiming to develop a load model that more accurately represents high-density crowd behavior.

First, step-frequency synchronization is the primary source of enhanced collective dynamic behavior under high-density conditions. A crowd synchronization coefficient ρ $(0 \le \rho \le 1)$ is defined to quantify the degree of convergence in pedestrian step frequencies: a larger ρ indicates greater synchronization. The synchronized step-frequency distribution can be expressed as:

$$f_i^* = f_i + \rho(f_0 - f_i) \tag{4}$$

where f_0 is the average step frequency of the crowd, and f_i is the free step frequency of the ith pedestrian. When $\rho \to 1$, the step frequencies of all pedestrians tend to converge; when $\rho \to 0$, the model reduces to the traditional independent random form.

Furthermore, to account for the feedback effect of structural vibrations on pedestrian gait, a coupling coefficient β (with a value range of 0–0.3) is introduced to describe this weak coupling mechanism. The adjusted step frequency is then defined as:

$$f_i^{**}(t) = f_i^* + \beta \cdot \Psi(u(x_i(t), t), \dot{u}(x_i(t), t)) \tag{5}$$

where u and $\dot{u}$ are the displacement and velocity of the structure at the pedestrian's location $x_i(t)$, respectively, and Ψ is the feedback function.

Based on the adjusted step frequency $f_i^{**}(t)$, the basic excitation force generated by pedestrian i is given by:

$$F_i^{base}(t) = G_i \sum_{h=1}^{N_h} \alpha h, i \, \sin(2\pi h f_i^{**}(t)t + \phi_{h,i}) \tag{6}$$

Considering the synchronization effect, the synchronized crowd excitation can be expressed as:

$$F_{sync}(x, t) = \sum_{i=1}^{N} F_i^{base}(t)\delta(x - x_i(t)) \tag{7}$$

Next, to account for the spatial correlation of footfall impacts between adjacent pedestrians, a coherence function is defined:

$$C(r) = e^{-r/L_c} \tag{8}$$

Where r is the distance between two pedestrians, and L_c is the coherence length. The multi-pedestrian coherent excitation can be expressed as:

$$F_{coh,i}(t) = \frac{1}{N} \sum_{j=1, j\neq i}^{N} C(|x_i(t) - x_j(t)|) \cdot F_j^{base}(t) \tag{9}$$

The spatial distribution of the coherent excitation is given by:

$$F_{coh}(x, t) = \sum_{i=1}^{N} F_{coh,i}(t)\delta(x - x_i(t)) \tag{10}$$

The final coupled multi-pedestrian excitation is expressed as:

$$F_{coupled}(x, t) = \sum_t F_i^*(x, t) \tag{11}$$

By integrating the above mechanisms, a comprehensive CSI model is established:

$$F_{total}(x, t) = \sum_{i=1}^{N} \left[G_i \sum_{h=1}^{N_h} \alpha_{h,i} \, \sin(2\pi h f_i^{**}(t)t + \varphi_{h,i}) + \frac{1}{N_p(t)} \sum_{j=1, j\neq i}^{N_p(t)} C(r_{ij}(t) \cdot F_j^{base}(t) \right] \cdot \delta(x - x_i(t)) \cdot W_i(t) \tag{12}$$

Where:

$$W_i(t) = H(t - \tau_i) - H\left(t - \tau_i - \frac{L_{WP}}{v_i}\right) \tag{13}$$

According to the Euler–Bernoulli beam theory, the dynamic equation is:

$$m\ddot{p}(x, t) + c\dot{p}(x, y) + EI\frac{\partial^4 p(x, t)}{\partial x^4} = \mathrm{F}_{\mathrm{total}}(x, t) \tag{14}$$

Where $x \in [0\ Lx]$ are the coordinates of a point on the wooden boardwalk, $\dot{p}$ is the speed, $\ddot{p}$ is the acceleration, E is the elastic modulus of the material, I is the moment of inertia of area.

In order to predict the vibration characteristics of the suspended structure under the load of tourists and ensure its safety and comfort, we need to calculate the deformation of the structure under the load. By using the beam structure to represent the dynamic response of the tourist load to the suspended structure, according to the modal decomposition method, the vertical deflection can be expressed as:

$$\mathrm{p}(x, t) = \sum_{j=1}^{\infty} \varphi_j(x) q_j(t) \tag{15}$$

Where q is vertical deflection, φ_j is the vibration, q_j is the generalized coordinate.

Assuming the damping is proportional, the acceleration dynamic response formula of the structure is:

$$\mathrm{M}\ddot{p}_{j,k}(t) + \mathrm{C}\dot{p}_{j,k}(t) + \mathrm{K}p_{j,k}(t) = F(x, t) \tag{16}$$

Where M is the mass matrix, C is the stiffness matrix, K is the damping matrix.

Random parameters

Considering the walking force of each tourist is different to one another, we next analyzed the randomness of the step excitation of different people in the normal walking process. From a probability perspective, the step frequency, step length, weight, dynamic load factor, etc., are regarded as random variables. They are all required to obey the normal distribution, which is defined as:

$$\begin{aligned} \mathrm{f_p} &\sim \mu_{\mathrm{f_p}}(1 + \mathrm{V_{f_p}N}(0, 1)) \\ \mathrm{v} &\sim \mu_{\mathrm{v}}(1 + \mathrm{V_c N}(0, 1)) \\ \mathrm{G} &\sim \mu_{\mathrm{G}}(1 + \mathrm{V_G N}(0, 1)) \\ a_{\mathrm{h}} &\sim \mu_{a_{\mathrm{h}}}(1 + \mathrm{V}_{a_{\mathrm{h}}}(0, 1)) \end{aligned} \tag{17}$$

Where μ and V represent the mean value and the coefficient of variation of the random variables, they all follow the standard normal distribution of N (0,1).

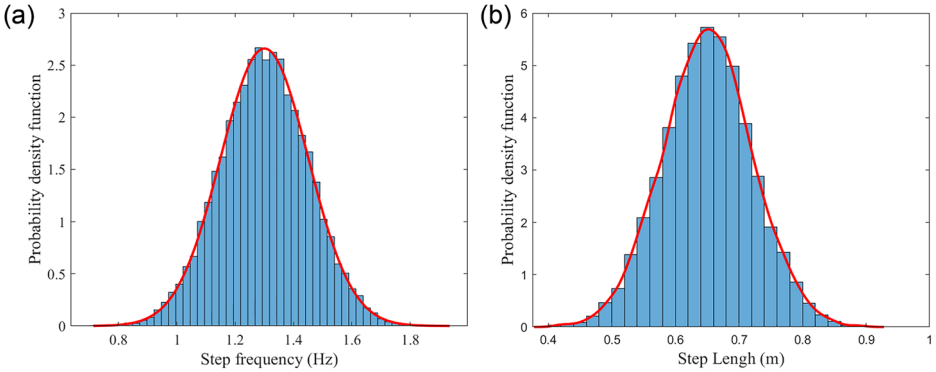

Fig. 6 | Probability density functions. a Walking frequency. **b** Step length.

The stochastic parameters are constrained according to the following specifications:

- The influence of step frequency on structural vibration response is particularly significant. The cadence of normal walking tourists is generally 1~3 Hz, which can be divided into three walking speeds: slow 1~1.6 Hz, medium 1.2~2.0 Hz, and fast 2~3 Hz[28]. Through on-site investigations and surveillance video analysis, it was found that tourists walked relatively slowly on the wooden boardwalk. Therefore, this paper sets the tourists' step frequency to follow the normal distribution $f_p \sim \mathrm{N}\ (1.3, 0.15^2)$ (Hz).
- Step frequency and step length can be approximately considered as two independent random variables. Walking speed can be calculated through these two parameters generated by Gaussian distribution. From the results of applying the Gaussian distribution, we can then calculate walking speed. In addition, the literature also points out that walking speed is linearly related to step frequency[29]. Therefore, this paper assumes that step length follows a normal distribution with a mean of 0.65 m and a standard deviation of 0.070 m, as shown in Fig. 6. The normal distribution of walking speed is $V \sim N\ (0.845, 0.1338^2)$.
- We assume that the phase angle distribution follows a uniform distribution of $\varphi_h \sim U\ (0, 2\pi)$.
- The weight of tourists follows a normal distribution with a mean of 75 kg and a standard deviation of 15 kg[30], $G \sim X\ (75,15)$.

Even when walking at the same step frequency, different individuals can generate different dynamic load factors. This study employs the classical Bachmann model to determine the dynamic load factor for each harmonic order. The model, established based on extensive field measurement data, calculates the factor using the following formula:

$$\begin{aligned} \alpha_1 &= 0.41(f_p - 0.95) \\ \alpha_2 &= 0.069 + 0.0056 f_p \\ \alpha_3 &= 0.033 + 0.0064 f_p \end{aligned} \tag{18}$$

For the synchronization coefficient, ρ: Based on observational studies of dense crowds, this study sets $\rho = 0.2$ for the primary analysis.

The coherence length, L_c, which relates to the perceived distance between pedestrians, typically ranges between 1 and 3 metres; here, $L_c = 2$ m is adopted.

The coupling coefficient, β, is treated in this work as a conceptual parameter aimed at qualitatively revealing the potential influence of the human–structure feedback mechanism; a value of $\beta = 0.15$ is used in the analysis.

Numerical analysis: Monte Carlo simulations

100 simulations of the dynamic response of random pedestrian loads were carried out in MATLAB. To ensure consistency between the static and dynamic analyzes, both the ABAQUS and MATLAB models were developed based on the same geometry, material parameters, and boundary conditions. In the ABAQUS model, the timber walkway and transverse beams were modeled using solid elements to accurately capture local stress and deformation under static loads. However, compared with solid elements, the number of degrees of freedom in the beam-element model grows exponentially slower, which is essential for reducing computational cost in large-scale Monte Carlo simulations that require numerous iterations. The timber walkway primarily undergoes bending and shear deformations, which are well aligned with the fundamental assumptions of beam theory. Therefore, to simplify the geometric representation and improve computational efficiency, the structure was idealized as a transverse–longitudinal beam lattice system in MATLAB. In this modeling system, the bridge deck is idealized as seven longitudinal girders arranged in parallel over the cross-beams, which are rigidly connected at the nodal points to form an integrated finite-element discretized system, as illustrated in Fig. 7. The railings are equivalently applied as a static load on the outermost nodes at the cantilever ends of the cross-beams. Subsequently, pedestrian walking loads, determined by the crowd density, are applied on the longitudinal girders to investigate the vertical dynamic response of the structure. Although the ABAQUS and MATLAB models differ in element types, their equivalence was ensured by maintaining consistent material properties, geometry, and boundary conditions. Consequently, the simplified beam-lattice model can reliably reproduce the overall dynamic behavior observed in the detailed solid-element model, providing an efficient and accurate foundation for the stochastic dynamic response analysis under pedestrian excitation. Assuming that the initial displacement of both the pedestrians and the structure is zero, Rayleigh damping was adopted in the analysis. The modal parameters and damping ratios of the timber walkway were obtained through on-site dynamic testing, with the measurement points and field layout shown in Fig. 8. A comparison between the modal frequencies and mode shapes derived from the finite element analysis and those measured in the field indicates good agreement, as summarized in Table 2. Specifically, the experimentally measured first and second natural frequencies are 3.257 Hz and 4.203 Hz, respectively, while the corresponding frequencies predicted by the finite element model are 3.963 Hz and 4.937 Hz, both within the acceptable range of engineering error. Moreover, the simulated and measured mode shapes exhibit a high degree of consistency in their dominant vibration patterns, particularly in the fundamental bending and torsional deformation modes of the wooden deck. These results validate that the developed finite element model can reliably capture the actual dynamic characteristics of the timber walkway, providing a credible numerical foundation for subsequent analyzes of dynamic responses under pedestrian loads.

The first two natural frequencies are selected as 3.26 HZ and 4.20 HZ, respectively. The damping ratio is 0.03, and the damping parameters α and β are determined[31].

$$\mathrm{C} = \alpha \mathrm{M} + \beta \mathrm{K} \tag{19}$$

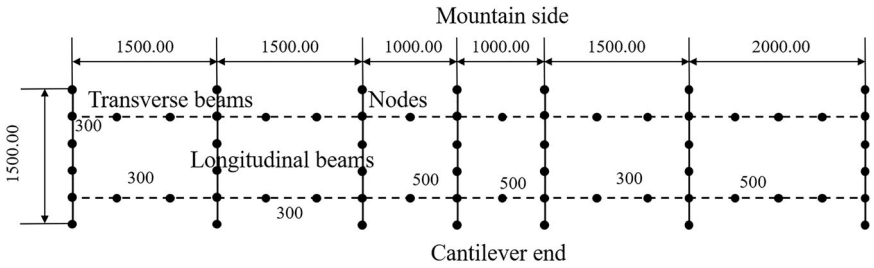

Fig. 7 | Finite Element Model. Schematic of the beam-element-based model developed in MATLAB.

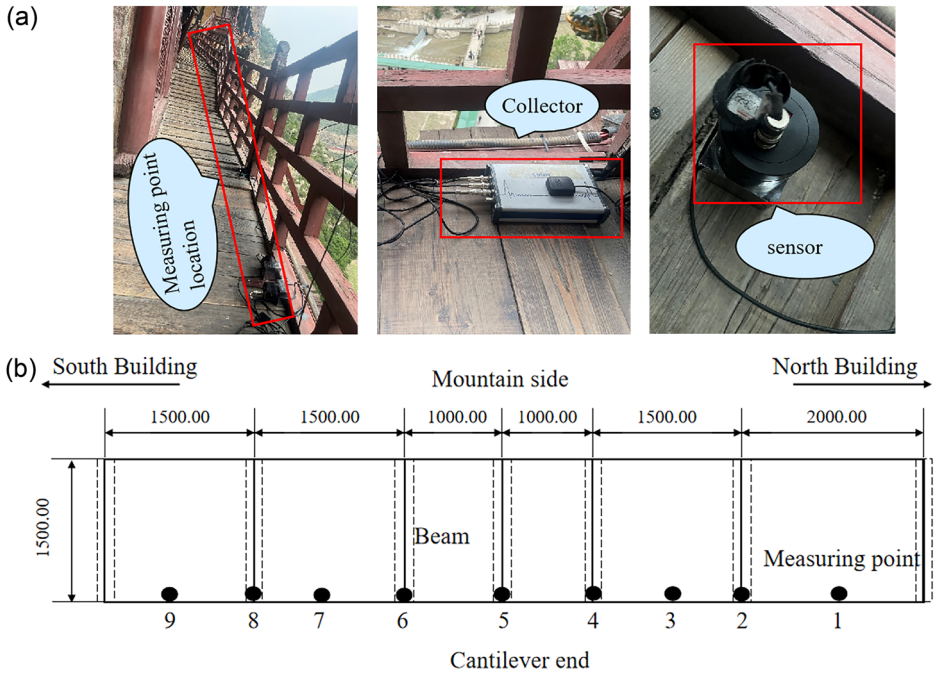

Fig. 8 | Schematic of the field dynamic testing arrangement. a Field test layout. **b** Measurement point layout.

Table 2 | Modal parameters

Degree	Modal (Hz)	Damping ratio (ζ)	Shaking type
1	3.257	0.030	
2	4.203	0.014	
1	3.963	—	
2	4.937	—	

$$a = \frac{2\omega_2\omega_3}{\omega_2+\omega_3}\zeta \tag{20}$$

$$\beta = \frac{2\zeta}{\omega_2+\omega_3} \tag{21}$$

The structural dynamic response was analyzed numerically using the Newmark-β method, with a focus on the mid-span vertical displacement and its time history at the monitored locations. The specific arrangement of the monitoring points is illustrated in Fig. 8. To further investigate the dynamic effects of visitor loads on the suspended ancient timber structure and considering the load-bearing capacity limit per unit area, this study defined four crowd-density scenarios in the load simulation: 1 person/m^2 (sparse), 2 persons/m^2 (moderate), 3 persons/m^2 (dense), and 4 persons/m^2 (over-dense).

Results

Static analysis under pedestrian load

To systematically evaluate the mechanical behavior and load-bearing capacity of the wooden boardwalk under crowd loading and to examine its safety margin under extreme conditions, four crowd-density scenarios were defined for vertical static graded loading analysis in this study: 1 person/m^2 (sparse), 2 persons/m^2 (moderate), 4 persons/m^2 (over-dense), and 6 persons/m^2 (ultimate loading). This design aims to systematically reveal the nonlinear evolution patterns of structural response with increasing crowd density and to provide clear graded loading benchmarks for safety assessment. As shown in Table 3, the loading test results of the wooden boardwalk under different crowd densities show that its stress and displacement are always within the design allowable range. Both the stress and displacement of the wooden walkway exhibit a significant increase with rising pedestrian density. Under Condition 1 (with supporting columns), displacement grows from 1.15 mm to 4.27 mm and stress from 0.06 MPa to 0.21 MPa as density increases from 1 to 6 persons/m^2. This moderate growth indicates that the columns effectively distribute the load, reducing overall deformation and stress concentration. In contrast, Condition 2 (without columns) results in consistently higher displacement and stress, with a peak displacement of 5.19 mm, indicating a noticeable reduction in structural stiffness and load-bearing capacity. Overall, the supporting columns substantially enhance the mechanical performance, particularly at high pedestrian densities (4–6 persons/m^2), by restraining excessive deformation and mitigating stress, thereby improving structural stability and safety. Figure 9 illustrates the displacement and stress contour distributions under a crowd load of 6 persons/m^2. The extreme displacement values for both conditions occur at the mid-span region of the timber deck, while the maximum stress is concentrated at the connection between the timber beam and the mountain body, exhibiting an increasing trend along the cliff wall direction.

Table 3 | Stress-displacement results under different population densities

conditions	Number of people	1 persons/m^2	2 persons/m^2	4 persons/m^2	6 persons/m^2
Condition 1	Displacement	1.15 mm	1.77 mm	2.99 mm	4.27 mm
	Stress	0.06 MPa	0.09 MPa	0.15 MPa	0.21Mpa
Condition 2	Displacement	1.37 mm	2.16 mm	3.02 mm	5.19 mm
	Stress	0.05 MPa	0.07 MPa	0.15 MPa	0.16 MPa

Dynamic analysis with random loads

As shown in Fig. 10a, as the crowd density increases from 0 to 4 persons/m^2, the maximum vertical accelerations predicted by both the stochastic model and the integrated model exhibit a monotonic upward trend. In the low-density range (1–2 persons/m^2), the peak accelerations predicted by the stochastic model are significantly higher than those from the integrated model. In the high-density range (3–4 persons/m^2), the results of the two models gradually converge and essentially coincide near 4 persons/m^2. It can be observed that, in the low-density stage, the stochastic model tends to overestimate peak accelerations due to statistical superposition while neglecting human–structure interaction constraints. In the high-density stage, synchronized pedestrian behavior becomes dominant, leading to similar characterizations of the equivalent excitation across different models, and thus a convergence in predictions. To verify the reliability of the models, field tests under pedestrian-induced excitation were conducted at the monitoring points on site. Restricted by visitor flow control in the scenic area, the measured data were mainly collected under low-density conditions (0.5, 1.0, and 1.5 persons/m^2). As shown in Fig. 10b, the measured average peak accelerations are 0.17 m/s^2, 0.26 m/s^2, and 0.38 m/s^2, respectively. These results align more closely with the predictions of the integrated model, indicating that the integrated model can reasonably reflect human–structure interactions under low crowd densities. Moreover, its convergent trend with the stochastic model at high densities reflects a

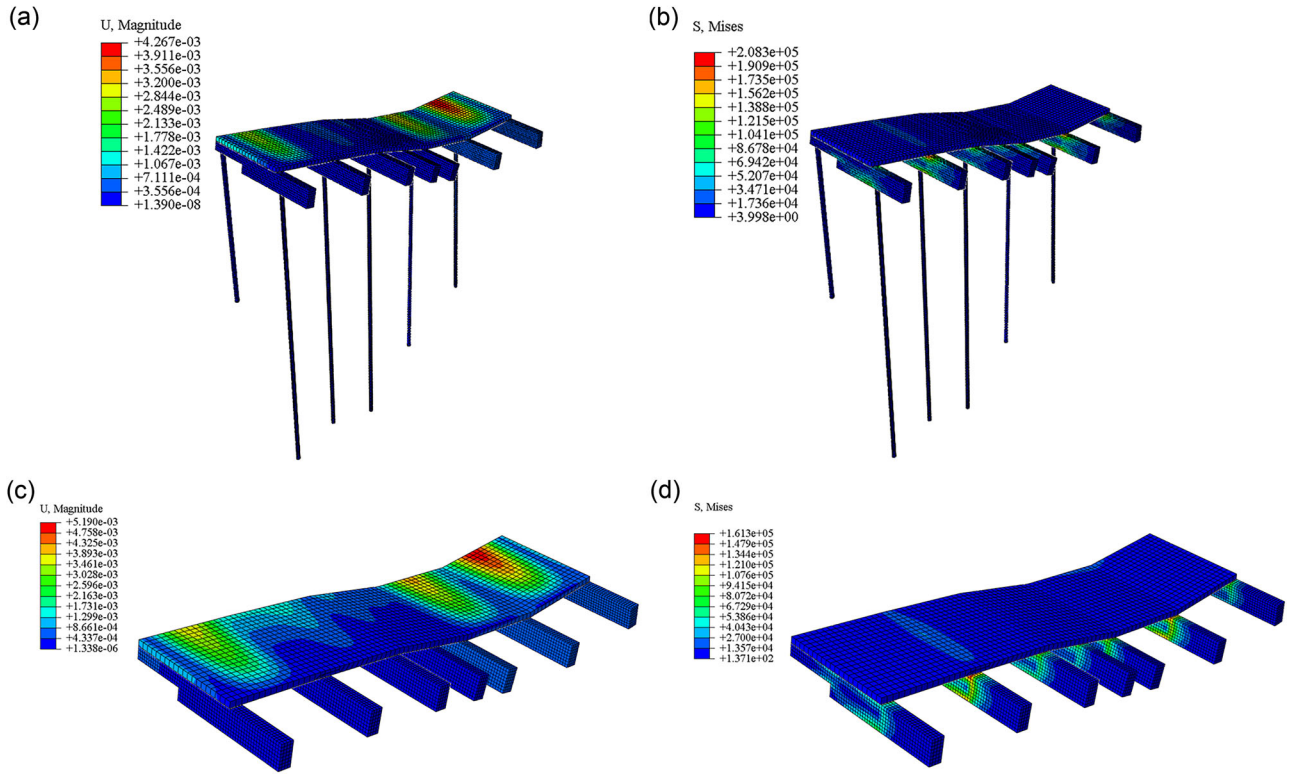

Fig. 9 | Comparative distributions of displacement and stress at 6 persons/m^2. a Displacement cloud map for Condition 1. **b** Stress cloud map for Condition 1. **c** Displacement cloud map for Condition 2. **d** Stress cloud map for Condition 2.

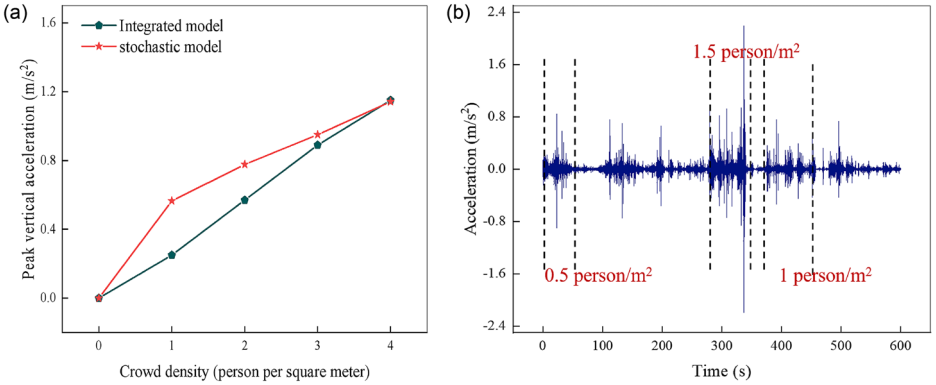

Fig. 10 | Acceleration response curve. a Mean value of maximum vertical acceleration response. **b** On-site acceleration measurements during normal tourist walking.

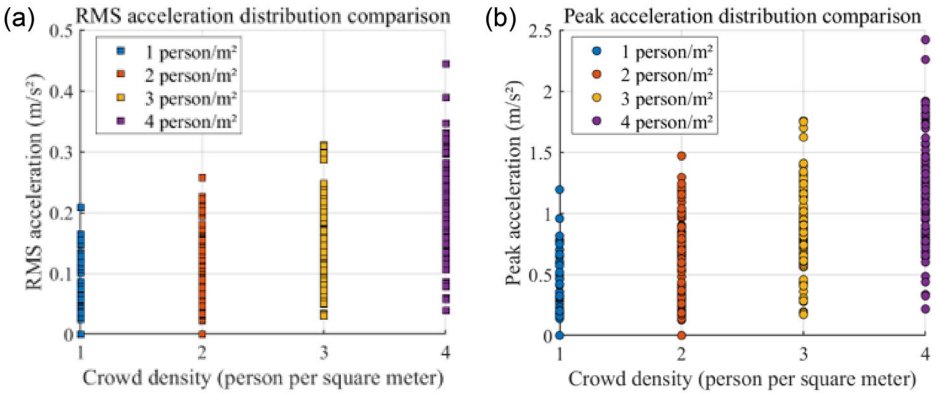

Fig. 11 | Acceleration distribution. a RMS acceleration distribution comparison. **b** Peak acceleration distribution comparison.

physically sound representation of group synchronization and coupling mechanisms, thereby validating the reliability and predictive superiority of the integrated model across the full density range.

RMS acceleration reflects the accumulated level of vibration energy rather than instantaneous peaks. The distribution results in Fig. 11a indicate that as crowd density increases, the overall vibration energy level of the structure rises. At medium densities, although the energy input from the crowd increases, structural damping and modal energy dissipation can still partially dissipate this energy. Under high-density conditions, the duration of pedestrian excitation is prolonged, and the effective number of participants in vibration increases, causing the structural vibration energy to accumulate more easily in a statistical sense, thereby amplifying the RMS response and its variability. This suggests that high crowd density not only elevates the average vibration level but may also significantly increase the uncertainty of structural vibration response, which has important implications for comfort and serviceability assessments.

The distribution results in Fig. 11b show that increasing crowd density notably raises the likelihood of extreme dynamic responses in the structure. Particularly under high-density conditions, although most response samples remain within an acceptable range, a small number of simulated results exhibit significantly amplified peak responses. This highlights the need to focus on low-probability, high-risk scenarios in safety evaluations.

As shown in Fig. 12, the acceleration time-history responses under four crowd density conditions indicate that the structural vibration is consistently dominated by a frequency component of ~3.25 Hz, which matches the first natural frequency of the structure. This confirms that the structural response is primarily governed by the fundamental mode across all density levels. As crowd density increases, the peak, mean, and RMS (root mean square) values of the response signal show a systematic rise, while the response dispersion band (the ±1 standard deviation interval) gradually widens. This reflects an overall increase in both the vibrational energy and the fluctuation range of the structure with higher density.

Under low-density (sparse crowd) conditions, the structural response exhibits forced vibration dominated by the first mode, with weak interaction among pedestrian step frequencies. The excitation can therefore be approximated as a superposition of independent random inputs. As density increases, the widening of the dispersion band suggests that interaction among pedestrian step frequencies begins to emerge. Statistically, the step frequencies of some pedestrians approach the fundamental frequency of the structure, thereby enhancing the sustained excitation of this mode. Concurrently, the average response amplitude rises significantly. The multiple simulated response curves form a distinct "band-like" distribution around the mean, with waveforms becoming more regular and random noise characteristics diminishing—indicating a gradual strengthening of step-frequency synchronization.

With further density increase, the excitation from adjacent pedestrians exhibits stronger temporal and spatial correlation. The combined effect of spatial coherence and step-frequency synchronization allows the main structural mode to receive continuous energy input, leading to a quasi-resonant state. At this stage, the average response waveform becomes highly regular. Despite the larger dispersion band, the vibration remains locked near 3.25 Hz. This implies that the structural vibration has begun to influence pedestrian gait, causing some pedestrians to adjust or lock their step frequencies, thereby establishing a weak human–structure coupling feedback mechanism that further reinforces the excitation of the first mode.

In summary, the increase in crowd density does not alter the inherent dynamic characteristics of the structure. Instead, it progressively amplifies the excitation intensity on the fundamental mode through three mechanisms: step-frequency synchronization, spatial coherence, and weak human–structure coupling. This observed behavior is consistent with the predictions of the established crowd–structure interaction model, validating its physical rationality under high-density crowd excitation.

According to the evaluation of vibration comfort based on the EU HiVoSS guidelines in Table 4, the results shown in Fig. 13 indicate that: at a

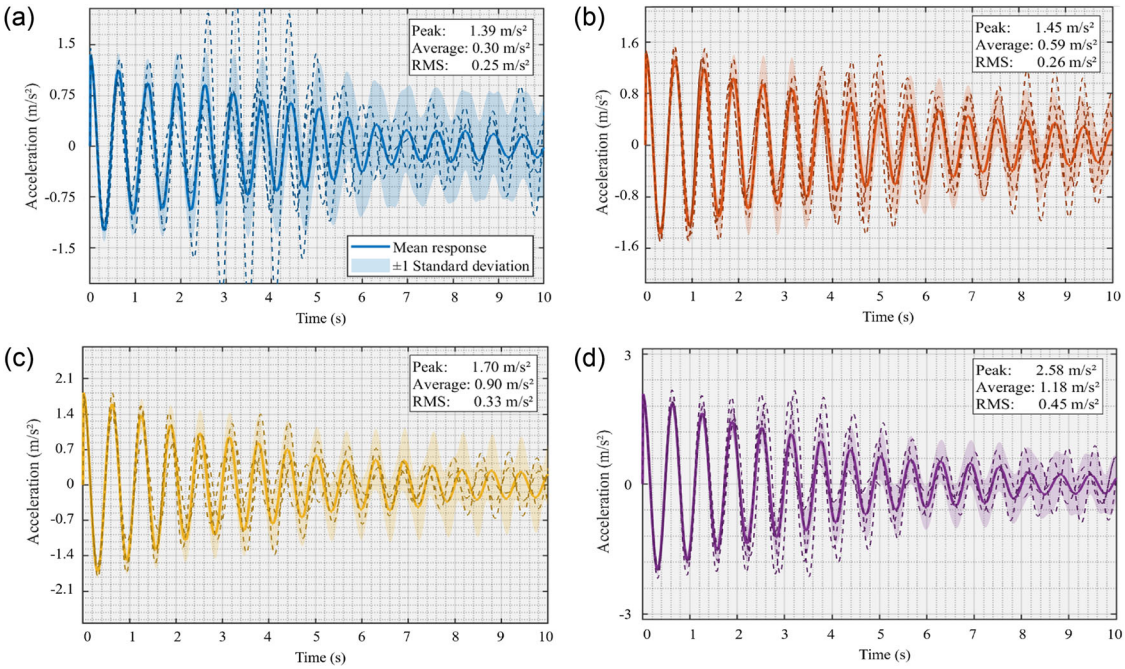

Fig. 12 | Acceleration response time history curve. a Population density 1 person/m^2. **b** Population density 2 person/m^2. **c** Population density 3 person/m^2. **d** Population density 4 person/m^2.

Table 4 | Vibration comfort criteria

Comfort level	Excellent	Good	Fair	Unacceptable
Horizontal acceleration	<0.1	0.1–0.3	0.3–0.8	>0.8
Vertical acceleration	<0.5	0.5–1.0	1.0–2.5	>2.5

crowd density of 1 person/m^2, the structural vibration falls within the "Excellent" grade, with almost no discomfort perceived. When the density increases to 2 persons/m^2, the vibration response intensifies but remains in the "Good" category, meeting normal serviceability requirements. At a density of 3 persons/m^2, the average acceleration approaches 0.9 m/s^2, reaching the comfort threshold, where the superposition of crowd loads and step-frequency synchronization effects become significant. When the density rises to 4 persons/m^2, the average acceleration reaches about 1.15 m/s^2, entering the "Acceptable" range. At this point, vibration perception is distinct, comfort decreases noticeably, and the structural service performance approaches the comfort limit, indicating potential risks.

Figure 14 shows the fluctuation of peak displacement under multiple conditions due to the randomness of pedestrian walking loads. In order to more accurately describe the complex nonlinear dynamic effects of the system's displacement response with varying numbers of pedestrians and to rapidly evaluate the wooden boardwalk, a cubic polynomial model was adopted to fit the peak displacement, thereby establishing a parametric prediction model. Specifically, the formula for fitting peak displacement under multiple-person random discrete walking loads is expressed as follows:

$$y = 2.11573^{-5}x^3 - 0.00263\,x^2 + 0.15429\,x + 0.4234 \qquad (22)$$

The goodness of fit of the model was assessed by its R^2 value of 0.95, indicating that the fitted curve explained the data variation well.

According to the Chinese standard GB 50005-2017 for timber structures, the deflection of flexural members must comply with specified limits. The wooden gallery in this study serves a structural function equivalent to "floor joists and beams" as defined in the code, with a prescribed deflection limit of l/250 (where l is the calculation span of the member). This value represents the fundamental requirement for evaluating structural stiffness and ensuring safe usage. However, as a heritage structure directly subjected to pedestrian loads, the wooden boardwalk of the Xuankong Temple functions more similarly to a footbridge and is particularly sensitive to vibrations. To ensure user comfort, prevent noticeable vibration-induced discomfort among visitors, and address the special conservation requirements of heritage buildings, engineering practice generally adopts more stringent deflection control criteria. Therefore, this study employs a tiered evaluation system for comprehensive assessment:

- Basic requirement: The calculated deflection must satisfy the mandatory code limit of l/250 to guarantee structural safety.
- Comfort requirement: To achieve superior user experience and higher safety redundancy, it is recommended to concurrently meet a recommended limit of l/400, which effectively controls structural vibration.

This tiered approach not only fulfills the mandatory provisions of the code but also reflects advanced concepts in the refined conservation of heritage structures and human-centered design. Based on this, it can be concluded that a deflection of $\omega < 12$ mm at the monitoring point represents the basic limit for structural safety, while $\omega < 7.5$ mm corresponds to the requirement for pedestrian comfort. According to the occupant-displacement fitting curve, when the crowd density reaches 4 persons/m^2, the peak displacement reaches 6.43 mm, approaching the comfort limit. This indicates a degradation in visitor experience and suggests potential safety risks.

Discussion

This study addresses the issue of dynamic response prediction and safety assessment of suspended ancient timber structures under tourist walking loads. By integrating field tests, numerical simulation, and theoretical modeling, it systematically investigates static graded loading, pedestrian load modeling, dynamic response prediction, and comfort evaluation. The main conclusions are as follows:

(1) Static graded loading tests reveal that although timber columns do not significantly share the stress of the main beams, they effectively restrain structural displacement. At a crowd density of 6 persons/m^2, the

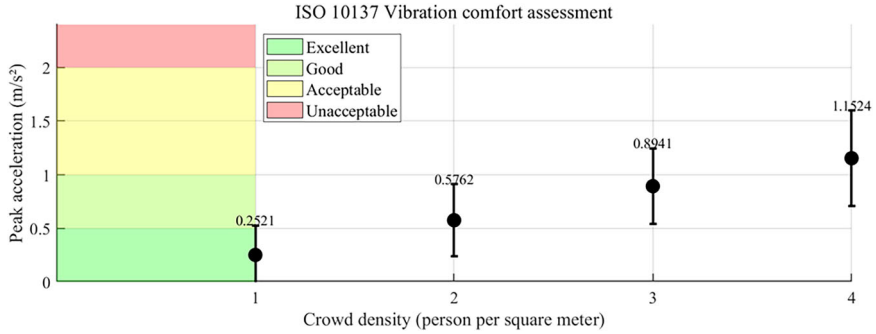

Fig. 13 | Comfort rating. ISO 10137 Vibration comfort assessment.

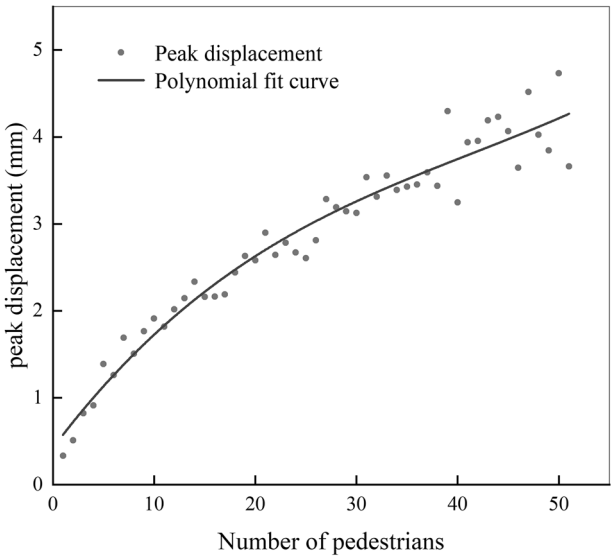

Fig. 14 | Number of people-displacement fitting curve. Used to predict peak displacement under crowd loading.

maximum displacement for the condition with columns (4.27 mm) is ~17.7% lower than that for the condition without columns (5.19 mm). This confirms the important safety redundancy function of timber columns in controlling overall structural deformation and enhancing deformation controllability.

(2) The integrated model, which incorporates step-frequency synchronization, spatial coherence, and weak human–structure coupling mechanisms, demonstrates high predictive accuracy across the full density range (0.5–4 persons/m^2). Its predictions show good agreement with measured data, significantly outperforming the traditional stochastic model. In the high-density stage, the results of the two models converge due to the dominant role of synchronization effects, validating the integrated model's reasonable representation of group synchronization and coupling mechanisms.

(3) As crowd density increases, the peak, mean, and RMS values of structural acceleration response show a systematic increase, indicating significant accumulation of vibration energy. When the density exceeds 3 persons/m^2, the average acceleration approaches 0.9 m/s^2, reaching the comfort threshold. At a density of 4 persons/m^2, the average acceleration is about 1.15 m/s^2, where comfort decreases noticeably, and structural service performance approaches the safety boundary.

This study follows the principle of non-destructive investigation and adopts an integrated research approach combining field monitoring, numerical simulation, and theoretical analysis. Although staged progress has been achieved in modeling crowd–structure interaction and conducting safety assessment of suspended ancient timber structures, several limitations remain, as discussed below:

First, constrained by practical considerations in cultural heritage preservation, it is currently difficult to carry out invasive tests or load tests on such precious heritage structures that may cause damage. As a result, in-depth experimental validation of the "safety redundancy" mechanism of timber columns is not feasible, and a systematic investigation into the applicability of Rayleigh damping parameters under higher-order vibration modes and varying crowd densities remains challenging. Additionally, existing research lacks directly comparable findings from similar structures. Second, although this study differentiates between structural safety and vibration comfort evaluation, in the vibration comfort analysis, non-structural components (such as wooden railings) are only included in the model as equivalent mass, without explicitly considering the subtle influence of their local stiffness on the overall dynamic characteristics. This simplifies the actual vibration propagation mechanism to some extent. Finally, current safety assessments primarily rely on static analysis and have yet to achieve real-time sensing and early warning of structural conditions.

Looking ahead, future research will be deepened in the following two directions:

(1) Refinement of models and mechanisms: Utilize long-term structural health monitoring data to continuously calibrate damping models and crowd–structure interaction models; where conditions permit, experiments on similar structures or full-scale tests may be conducted to further elucidate the collaborative working mechanisms of timber columns and other components.

(2) Development of an intelligent monitoring and early warning system: Integrate technologies such as IoT sensing, computer vision, and machine learning to build an intelligent platform capable of vibration monitoring, crowd density identification, and safety status early warning. This will promote the transition of safety assessment from "post-event analysis" to "pre-warning," gradually establishing a new paradigm for heritage conservation characterized by "intelligent sensing – precise prediction – dynamic control".

Data availability

All figures in this manuscript are original and were created by the authors. The datasets generated and/or analyzed during the current study are not publicly available due to restrictions concerning the preservation and site security of the immovable cultural heritage involved. Detailed geometric, material, and structural weakness data could be misused if openly shared. However, they are available from the corresponding author on reasonable request. The custom MATLAB scripts and the Abaqus finite element model files developed for this study contain specific parameters and geometric details of the heritage structure. They are subject to a confidentiality agreement with the cultural heritage administration but are available from the corresponding author on reasonable request for academic or preservation purposes, subject to a formal data-sharing agreement. The commercial software used were MATLAB R2022a and Abaqus 6.14. Key parameters (including material properties, boundary conditions, and load

combinations) required to interpret the findings are provided in the Methods section.

Code availability

The custom MATLAB scripts and the Abaqus finite element model files developed for this study contain specific parameters and geometric details of the heritage structure. They are subject to a confidentiality agreement with the cultural heritage administration but are available from the corresponding author on reasonable request for academic or preservation purposes, subject to a formal data-sharing agreement. The commercial software used were MATLAB R2022a and Abaqus 6.14. Key parameters (including material properties, boundary conditions, and load combinations) required to interpret the findings are provided in the Methods section.

Received: 25 July 2025; Accepted: 13 January 2026;
Published online: 24 January 2026

References

1. Rezende, F. et al. Evaluation of TMD performance in footbridges using human walking probabilistic models. *Vibration* **4**(2), 323–340 (2021).
2. Samuel, A. et al. Durability and protection of mass timber structures: a review. *J. Build. Eng.* **46**, 103731 (2022).
3. Muhammad, Z. O. & Reynolds, P. Probabilistic multiple pedestrian walking force model including pedestrian inter-and intrasubject variabilities. *Adv. Civ. Eng.* **2020**(1), 9093037 (2020).
4. Cheraghi-Shirazi, N., Crews, K. & Malek, S. Review of vibration assessment methods for steel-timber composite floors. *Buildings* **12**(12), 2061 (2022).
5. Figueiredo, F. et al. A parametric study of composite footbridges under pedestrian walking loads. *Eng. Struct.* **30**(3), 605–615 (2007).
6. Song Z. G. & Jin W. L. Peak acceleration response spectrum of long span floor vibration by pedestrian excitation. *J. Build. Struct*. **2004**(02), 57–63+98 (2004).
7. Chen, J., Xu, R. & Zhang, M. Acceleration response spectrum for predicting floor vibration due to occupant walking. *J. Sound Vib.* **333**(15), 3564–3579 (2014).
8. Wang, J., Chen, J. & Yokoyama, Y. Spectral model for crowd walking load. *J. Struct. Eng.* **146**(3), 04019220 (2020).
9. Basaglia, B. M., Li, J., Shrestha, R. & Crews, K. Response prediction to walking-induced vibrations of a long-span timber floor. *J. Struct. Eng.* **147**(2), 04020326 (2021).
10. Bayat, E. & Tubino, F. Dynamic response of floors induced by a single walking pedestrian including walking path variability. *Structures* **46**(2022), 1280–92 (2022).
11. Cristoforo, D., Maria, A. A. & Francesco, R. Deterministic and probabilistic serviceability assessment of footbridge vibrations due to a single walker crossing. *Shock Vib.* **2018**(2018), 1–26 (2018).
12. Picozzi, V., Avossa, A. & Ricciardelli, F. Probabilistic assessment of footbridge response to single walkers. *Arch. Appl. Mech.* **92**(6), 1913–27 (2022).
13. Abdeljaber, O. et al. A novel video-vibration monitoring system for walking pattern identification on floors. *Adv. Eng. Softw.* **139**(2020), 102710 (2022).
14. Zhang, X. et al. Vibration of a U-shaped steel–concrete composite hollow waffle floor under human-induced excitations. *Adv. Struct. Eng.* **23**(14), 2996–3008 (2020).
15. Wang, C. & Shi, W. Optimal design and application of a multiple tuned mass damper system for an in-service footbridge. *Sustainability* **11**(10), 1–20 (2019).
16. He, W. & Xie, W. Characterization of stationary and walking people on vertical dynamic properties of a lively lightweight bridge. *Struct. Control Health Monit.* **25**(3), 1–24 (2018).
17. Wang, C. et al. Predicting the human-induced vibration of cross laminated timber floor under multi-person loadings. *Structures* **29**(2021), 65–78 (2021).
18. Wang, J. et al. Spectral model for crowd walking load. *J. Struct. Eng.* **146**(3), 04019220 (2020).
19. Mao, X. et al. Analysis of flood resistance of masonry arch bridges combining numerical simulation and probabilistic analysis. *Int. J. Archit. Herit.* **19**(10), 1–14 (2024).
20. Georgakis, C. T. & Ingólfsson, E. T. Vertical footbridge vibrations: the response spectrum methodology. *Proc. 3rd Int. Footbridge Conf.* **2008**(2008), 267–275 (2008).
21. Piccardo, G. & Tubino, F. Equivalent spectral model and maximum dynamic response for the serviceability analysis of footbridges. *Eng. Struct.* **40**(2012), 445–456 (2012).
22. Bayat, E. & Tubino, F. Probabilistic assessment of the dynamic response of floors under multi-pedestrian walking loads. *Mech. Syst. Signal Process.* **213**, 111363 (2024).
23. Marta, G. et al. Bespoke footbridge for studying pedestrian–structure interaction with vertical vibration. *J. Bridge Eng.* **30**(1), 11363 (2025).
24. Zhang, R. et al. A virtual reconstruction method for corridor gable buildings based on the knowledge of structural dynamics: taking Leiyin Cave as an example. *Herit. Sci.* **12**(1), 316 (2024).
25. David, S. et al. Apparent and resistant section parametric modelling of timber structures in HBIM. *J. Build. Eng.* **49**(2022), 103990 (2022).
26. Xu, F. et al. Experimental study on deformation characteristics of new prestressed subgrade under static and dynamic loads. *Constr. Build. Mater.* **447**, 138123 (2024).
27. Tang, Z. et al. Numerical analysis of impact resistance mechanical properties of energy-absorbing columns under static and dynamic loads. *Sci. Rep.* **14**(1), 25347 (2024).
28. He F. T. et al. Research on step length estimation method for indoor navigation based on fuzzy logic. *Electron. Technol. Appl*. **42**(11), 59–61+65 (2016).
29. Ingólfsson, E. T. et al. Experimental identification of pedestrian-induced lateral forces on footbridges. *J. Sound Vib.* **330**(6), 1265–1284 (2011).
30. Cao, D., Pan, Z. & Fang, Y. Dynamic response analysis of the floor structure under random crowd excitation. *Shock Vib.* **2024**(1), 1451839 (2024).
31. Liu, K. et al. Dynamic testing and numerical simulation of human-induced vibration of cantilevered floor with tuned mass dampers. *Structures* **34**, 1475–1488 (2021).

Acknowledgements

Thanks to the support of the Key Laboratory of Fine Reconstruction and Health Monitoring of Architectural Heritage. This research was funded by the National Key Research and Development Program of China [No. 2022YFF0904300], the National Natural Science Foundation of China [No. 42301516], and the BUCEA Doctor Graduate Scientific Research Ability Improvement Project [No. DG2025038]. and the Sponsored by Beijing Nova Program [No. 20250484997].

Author contributions

All authors contributed to the study conception and design. Material preparation, data collection and analysis were performed by M.H., X.L., Y.D., J.H., and Y.D. J.W. and X.B. provided the monitoring equipment and the monitoring methodology. The first draft of the manuscript was written by R.Z. and all authors commented on previous versions of the manuscript. All authors read and approved the final manuscript.

Competing interests

The authors declare no competing interests.

Additional information

Correspondence and requests for materials should be addressed to Youqiang Dong.